

Title no. 96-S41

# Experimental Study of Influence of Bond on Flexural Behavior of Concrete Beams Pretensioned with Aramid Fiber Reinforced Plastics

by Janet M. Lees and Chris J. Burgoyne

An experimental program was formulated to investigate the flexural behavior of concrete prestressed with aramid fiber reinforced plastic (AFRP) tendons. The particular focus was the influence of the bond between an AFRP tendon and concrete on the flexural response of a beam.

In the main test series, pretensioned concrete beams were cast using either one of two types of AFRP tendons or steel tendons. The influence of bond was studied by testing beams with fully-bonded tendons, unbonded tendons or partially-bonded tendons. It was found that, although the fully-bonded beams had a high ultimate load capacity, only limited rotation occurred prior to failure. In contrast, large rotations were noted in the unbonded beams, but the strengths of these members were significantly (25 percent) lower than those of the fully-bonded beams. The only beams that achieved both a high rotation capacity and a high ultimate load capacity were the beams with partially-bonded tendons.

It is suggested that the use of partially-bonded tendons could provide the basis of a new design method for concrete beams prestressed with fiber reinforced plastic (FRP) tendons.

**Keywords:** bond (concrete to reinforcement); flexural strength; prestressed concrete.

## INTRODUCTION

The social and financial costs associated with the repair of existing corrosion-damaged steel reinforced concrete infrastructure are high. In the U.K., the Department of Transport has only recently lifted a 4-year ban on the use of grouted steel prestressing tendons. The ban had been imposed because of fears of the tendons corroding and the difficulties associated with the detection of this type of deterioration. The problems associated with steel corrosion are most severe in countries where road deicing salts are used extensively. The construction industry needs to seek alternatives to steel reinforcement; a potential solution is the use of fiber reinforced plastics (FRPs) as concrete reinforcement.

The term fiber reinforced plastics describes a group of materials composed of inorganic or organic fibers embedded in a resin matrix. FRPs are lightweight, strong, nonmagnetic, and, for the most part, noncorrodible. It is the last property that is particularly attractive to designers.

In the construction industry, the most commonly used FRPs are glass fiber reinforced plastics (GFRPs), carbon fiber reinforced plastics (CFRPs) and aramid fiber reinforced plastics (AFRPs). Fig. 1 shows typical stress-strain properties of these three materials and steel. The focus of the present study is AFRPs, but it is believed that the principles identified in the current work are applicable to all three types of FRP materials.

## RESEARCH SIGNIFICANCE

Conventional flexural design methods for steel-prestressed concrete members are based on the assumption that the steel will yield prior to the failure of the beam. When the steel yields,

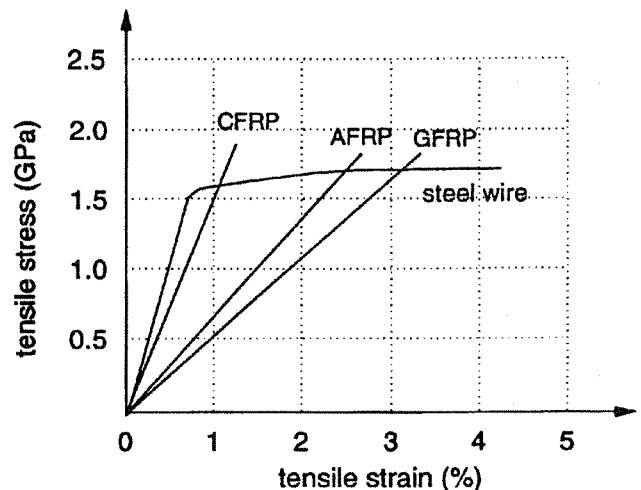


Fig. 1—Schematic stress-strain curves for different types of FRPs (within each category of FRP, materials will vary both in terms of strength and modulus of elasticity).

large deflections ensue and inelastic energy is absorbed. The absorption of inelastic energy results in a ductile structure.

FRP materials are linearly elastic and do not yield. Hence, the amount of plastic energy dissipated in an FRP system is much less than with a steel-prestressed system. As there is a high proportion of elastic energy in a structure with FRP reinforcement, it is essential that large rotations occur in these members to warn of pending failure.

The distinction between rotation capacity and ductility is important. The occurrence of large elastic rotations in a member prestressed with FRPs does not necessarily result in a ductile structure. Final failure due to rupture of the FRP tendons will be brittle and sudden, with large amounts of elastic energy being released. From a safety point of view, the necessity of a high rotation capacity in members with FRP tendons therefore becomes crucial.

The FRP industry had been producing tendons that were intended to look like reinforcing bars, and they were conducting tests to demonstrate the high bond capacities that could be achieved. Burgoyne<sup>1</sup> questioned the desirability of this approach. The aim of the study was to demonstrate the influence of the bond between the AFRP tendon and concrete on the rotation capacity of a concrete beam prestressed with AFRPs.

ACI Structural Journal, V. 96, No. 3, May-June 1999.

Received May 21, 1997, and reviewed under Institute publication policies. Copyright © 1999, American Concrete Institute. All rights reserved, including the making of copies unless permission is obtained from the copyright proprietors. Pertinent discussion will be published in the March-April 2000 ACI Structural Journal if received by November 1, 1999.

Janet M. Lees received her PhD from the University of Cambridge, UK, in 1997 where she is currently a lecturer. Her research interests include the use of fiber reinforced plastics in construction applications and the behavior of concrete structures.

Chris J. Burgoyne is a lecturer at the University of Cambridge, UK. He is a member of ACI Committee 440, Fiber Reinforced Polymer Reinforcement. His research interests include advanced composites applied to concrete structures.

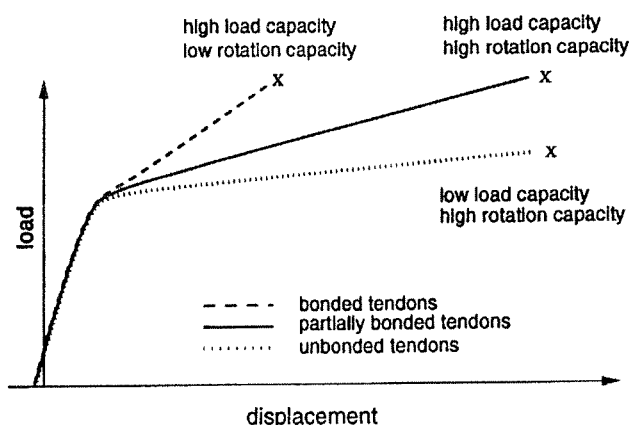


Fig. 2—Schematic load-deflection curves.

### INFLUENCE OF BOND

Before cracking occurs, the strains in the concrete are small and fairly uniform over the length of the beam, so the degree of bond has relatively little effect on the behavior of the beam. However, once cracking occurs in the concrete, the amount of bond can have a significant effect.

Beams with fully-bonded tendons must have the same change in strain in both the tendon and the concrete, except at the crack locations where there must be some breakdown of bond on either side of the crack. If the tendon can yield (as for steel tendons), high bond stresses do not cause a problem; the tendon carries its yield load and can stretch plastically to maintain compatibility. However, if the tendon cannot yield (as for FRP tendons), it will snap as soon as the strain reaches a limiting value. The result will be a high moment capacity, since the tendon reaches its failure load, but limited rotation capacity.

With unbonded or external tendons, the tendon is free to slide relative to the concrete. The strain increase in the tendon due to the displacement is distributed fairly uniformly along the length of the tendon. Large rotations can be realized since the concrete can have a large strain at a few crack locations, while the tendon has a relatively low strain over its whole length. The corollary is that since the tendon's strain, and hence stress, are low, the moment capacity is reduced and the final failure is typically due to premature concrete crushing at one of the crack locations.

Thus, the idea of partial bond is to obtain the best of both worlds. There should be sufficient bond to allow the tendon to achieve its full strength, but the amount of bond must be limited to insure that the tendon can achieve high strains over a reasonable length before failure. Both a high ultimate load capacity and high rotation can then be achieved (Fig. 2).

In the current study, partial bonding was achieved in two ways; either by intermittently bonding sections of tendon, or by coating the tendon with a resin of known and low shear strength. Both of these types of partial bonding will be described.

### Intermittent bond

In this system, discrete lengths of FRP tendons are alternately bonded and debonded (Fig. 3). By intermittently debonding the tendon, the length over which the tendon can strain is controlled.

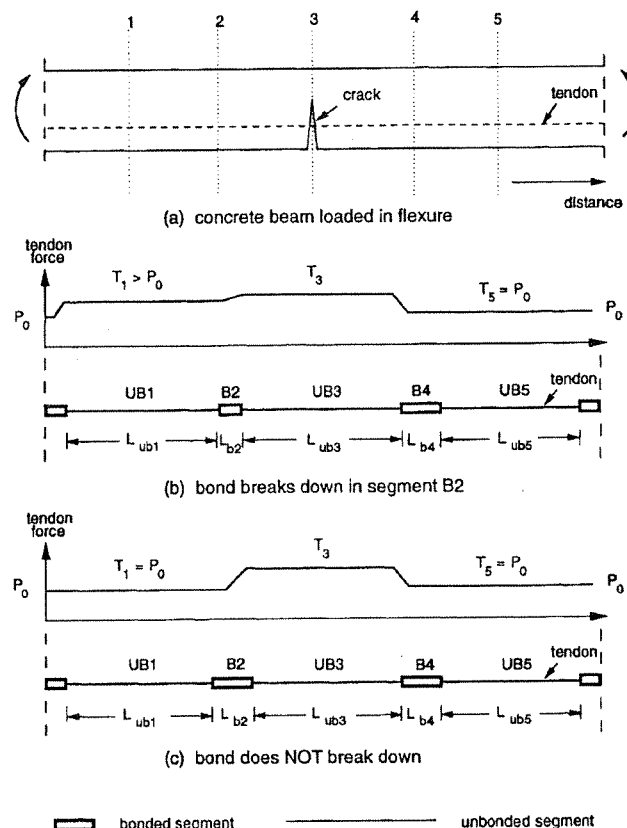


Fig. 3—Intermittently-bonded tendons.

Fig. 3(a) shows part of a concrete beam subject to a sagging-bending moment. A prestressing tendon that is alternately bonded (*B*) and unbonded (*UB*) to the concrete passes through this region. In general, the unbonded lengths will be longer than the bonded lengths.

In Fig. 3, the bonded sections are denoted by open boxes and are prefixed with *B*, whereas the unbonded sections are represented as a thin line and are prefixed with *UB*. A subscript is used to identify a particular tendon segment. The tendon forces *T* along the length of the tendon are also shown.

Before loading, the tendon forces in all the regions are equal to the initial prestress force  $P_0$ . When a load is applied, the compressive strain in the concrete decreases on the lower face until a crack forms. For the purposes of illustration, it will be assumed that this crack intersects Segment *UB3*; the force in this segment will increase to the level  $T_3$ .

The subsequent behavior depends on the length of the adjacent bonded segments. If the bonded lengths are insufficient to carry the difference between the ultimate capacity of the tendon and the initial prestress force, the bond will break down during loading [Fig. 3(b)]. Hence, the extent and distribution of the bonded sections can be designed so that when the force in a particular unbonded segment, i.e., *UB3*, approaches a predetermined threshold, the bond in an adjacent bonded segment, i.e., *B2*, will break down and force would be transferred to *UB1*. This type of controlled bond failure prevents any individual segment from becoming overstressed and causing a brittle failure, at least until the neighboring regions are fully stressed.

An alternative case arises if the bonded lengths are sufficient to transfer the difference between the ultimate capacity of the tendon and the initial prestress force; the bond will not then break down during loading [Fig. 3(c)]. Hence, in this scenario, even when the force in Segment *UB3* approaches the breaking load of the tendon, there is no transfer of force from *UB3* to *UB1*.

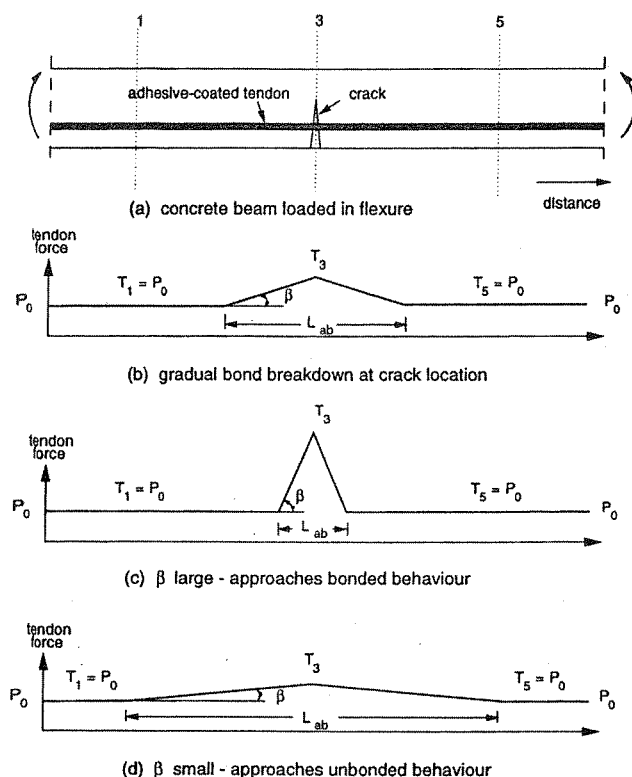


Fig. 4—Tendon coated with adhesive.

or from UB3 to UB5. The rotation at the crack location will be dependent only on the length of the unbonded region, UB3.

### Coating of tendon

Another possibility is to reduce the bond strength between the tendon and the concrete by coating the tendon with a resin adhesive. The properties of the resin should be such that only small bond stresses can be sustained, which controls the rate at which force can build up in the tendon along its length. As a result, when cracking occurs, the force in the tendon varies over a significant length on either side of the crack. The length required to transmit the additional force to the tendon is a function of the resin shear strength and is related to the angle  $\beta$ , as shown in Fig. 4. The angle  $\beta$  reflects the change in force with length, and the distribution of tendon force due to three different values of  $\beta$  are shown in Fig. 4 (a constant bond stress distribution has been assumed). In each case, the force  $T_3$  and the length  $L_{ab}$  vary, and the analysis is complex; the force  $T_3$  must satisfy overall equilibrium of the section, and the triangle of length  $L_{ab}$  and height  $T_3 - P_0$  is related to the additional extension of the tendon, which must satisfy overall compatibility conditions. This analysis will be described elsewhere.<sup>2</sup>

After transfer, the force in the tendon at Location 1, 3, and 5 are all equal to the initial prestress force  $P_0$ . If a crack occurs at 3, there will be an increase in the tendon force at this location. The rate that this force increase can be transmitted along the tendon is governed by the value of  $\beta$ , which will thus dictate the tendon length that is affected by the force increase.

The magnitude of  $\beta$  has an important influence on the behavior of the beam. If  $\beta$  is too large, then the strain near the crack occurs over only a small length of tendon and, although the increase in force is quite high, the extension of the tendon will be minimal. As a result, only small rotations will occur and the behavior of the beam will be similar to that of beams with fully-bonded tendons [Fig. 4(c)]. If the value of  $\beta$  is too small then, after first cracking, the tendon strains over such a long length that the flexural response becomes analogous to beams with

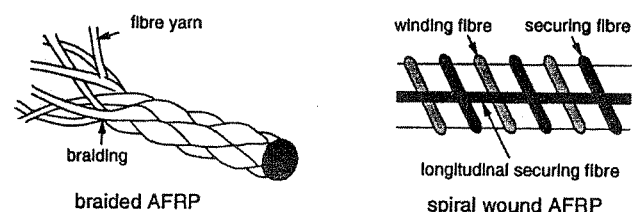


Fig. 5—AFRP rods after Nanni et al.<sup>3</sup> and Noritake et al.<sup>4</sup>

Table 1—Tendon and fiber material properties<sup>5-9</sup>

Material	Density, kg/m <sup>3</sup>	Fiber type	Young's modulus, GPa	Maximum elongation, percent	Tensile strength, MPa	$V_f$ , percent
Braided FiBRA	1.28	Kevlar 49	68.6	2.0	1480	65 to 70
Kevlar 49 fiber	1.45	Kevlar 49	120.0	2.5	2800	100
Spiral wound Technora	1.3	Technora	54.0	3.7	1900	65
Technora fiber	1.39	Technora	73.0	4.6	3400	100
Steel (high-yield)	7.8	N/A	200	10.0	650	N/A
Steel (prestress)	7.8	N/A	220	4.2*	1760	N/A

\*Measured value.

unbonded tendons. Although large rotations are realized, the moment capacity would be expected to be reduced [Fig. 4(d)].

Hence, a judicious choice of  $\beta$  is required that is low enough to insure large rotations, but large enough to insure that adequate forces develop at the crack interface. In this way, a distributed crack pattern will result, and the tendon will be able to achieve its full capacity prior to concrete crushing.

### TEST PROGRAM

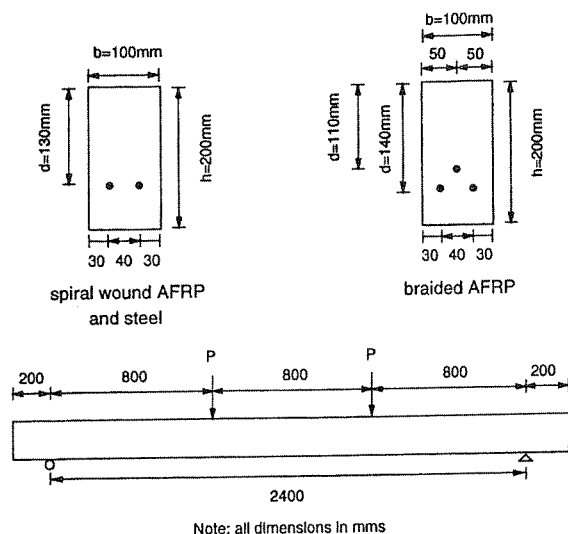
The main experimental program was designed to demonstrate the influence of the bond between an AFRP tendon and concrete on the flexural response of a pretensioned concrete beam. Beams with fully-bonded, unbonded and partially-bonded tendons were considered.

### Design philosophy

Concrete beams pretensioned with small-diameter AFRP tendons were cast and tested. Two types of AFRP tendon, a braided rod comprised of Kevlar 49 fibers in an epoxy resin (FiBRA), and a spiral wound pultrusion with Technora fiber in a vinylester matrix (Technora rod), were used (Fig. 5). Beams with steel tendons were included in the bonded and unbonded test series for comparison purposes. The properties of the three tendon materials can be found in Table 1.

The use of small-diameter tendons was deemed advantageous since specimen sizes could be kept to a minimum, and a pretensioned system was chosen since it avoided the need for long-term anchorages. However, the provision of even a temporary anchoring system proved to be problematic. A stressing system based on the use of expansive cement couplers was eventually chosen.<sup>10</sup>

It was proposed that the strands be tensioned to approximately 70 percent of their ultimate strength. A high proportion of the creep and relaxation experienced by the FRP tendons occurs soon after tensioning. It was therefore expected that, by the time the beams were tested, the tendons would be stressed to approximately 60 to 65 percent of their ultimate capacity. This seemed to be a practical level of prestressing and, in view of the time-scale of the experiments, long-term stress rupture would not be an issue at these levels of prestressing.<sup>11</sup>



Note: all dimensions in mm

Material	No. of tendons	$E_t$ (MPa)	Parameters for a single tendon		
			$\phi$ (mm)	area (mm <sup>2</sup> )	$P_{ult}$ (kN)
braided AFRP	3	68,600	3.7	11	15.7
spiral wound AFRP	2	54,000	4	12.6	22.7
steel	2	220,000	5	19.6	34.4

Fig. 6—Beam cross sections and loading arrangement.

To have similar ultimate load capacities for both AFRP beams, the beams with the braided AFRP contained three No. 3.7-mm diameter tendons, whereas the beams with the spiral wound AFRP contained two No. 4-mm diameter tendons. The beams with prestressing steel were stressed using two No. 5-mm diameter tendons that were part of the laboratory's stock. In each case, the centroid of the tendons was located in the middle third of the beam (Fig. 6). The section sizes (100 x 200 x 2800 mm) and prestress levels were the same in all cases, but the extent and distribution of the bond between the concrete and the tendon varied. All the beams were tested in flexure using a four-point loading arrangement (Fig. 6). For the partially-bonded beams, an 8-mm-high triangular crack inducer was included at the center of the beam, thereby reducing the beam depth at this section. This was primarily intended to fix the location of the first crack so that the beam could be properly instrumented.

The test series included beams with fully-bonded, unbonded, intermittently-bonded, and adhesive-bonded tendons. In all cases, the ends of the tendon remained bonded to the concrete to insure the integrity of the tendon anchorage.

### Fully-bonded and unbonded beams

The fully-bonded beams were designed to fail due to tendon rupture. In contrast, the unbonded beams, where the central portion of the tendon was debonded from the concrete, were expected to fail as a result of concrete crushing.

### Intermittently-bonded beams

The first series of intermittently-bonded beams were designed so that, as the force on one side of the bonded section reached a certain threshold, the bond would break down and the force would be transmitted to an adjacent length of tendon. This would be designed to occur before the more highly stressed element ruptured.

Based on the results of a series of prestressed pullout tests,<sup>12</sup> it was clear that a significant bond stress could be transmitted through very short bonded lengths of tendon. A bond length of

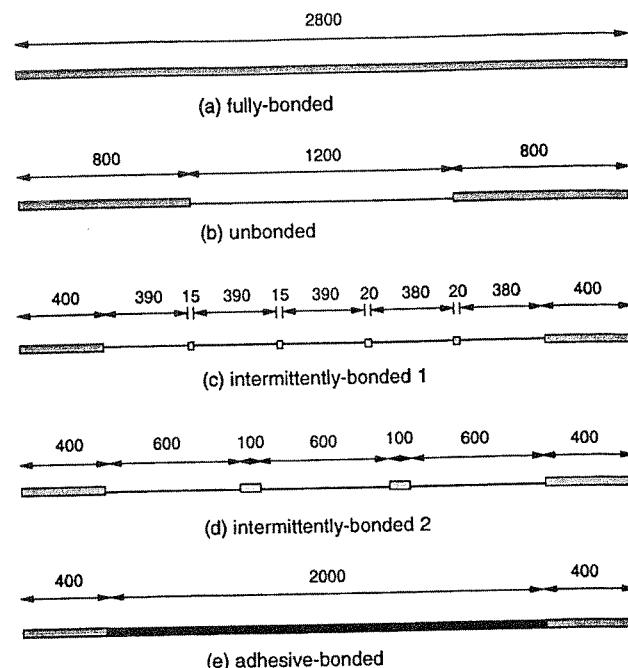


Fig. 7—Tendon details.

15 mm was chosen to encourage the bond to break down when the tendon reached a force of approximately  $0.80 P_{ult}$ , where  $P_{ult}$  is the breaking load of the tendon. To investigate possible effects due to an asymmetrical distribution of bond, the lengths of the bonded tendon segments on one side of the beam were increased to 20 mm [Fig. 7(c)].

In the second series of intermittently-bonded beams, the bonded lengths were much longer (100 mm) and more indicative of a length that would be considered in the design of a prototype beam [Fig. 7(d)]. However, as a result, the bond was unlikely to break down during testing and the tendon would snap, though at a larger rotation than for the fully-bonded beams.

### Adhesive-bonded beams

The goal of the adhesive-bonded tests was to determine the effect of limiting the bond between the tendon and the concrete by coating the tendon with a resin [Fig. 7(e)]. Tests were carried out to give initial insight into the bond strength of the adhesive.<sup>12</sup>

### Experimental procedure

The use of a rapid-hardening portland cement mix to obtain a high strength at an early age optimized the casting-testing program (a compressive cube strength of approximately 60 MPa was achieved after 7 days). Because of the low water cement ratio ( $w/c$ ) of 0.37, a superplasticizer was added to the mix to improve workability.

The casting rig was designed so that two beams could be cast at the same time (Fig. 8). The detensioning system was such that the prestress force would be released gradually.

The test setup was incorporated in a stiff reaction frame. The loads were applied using two 10-tonne (100 kN) hydraulic jacks, each with a 100-mm extension (Fig. 9).

### Experimental methodology

The AFRP tendons were prepared to suit the particular test series. The fully-bonded tendons required no treatment. For the unbonded and partially-bonded tendons, the unbonded regions were formed by covering the tendons in appropriate lengths of plastic tube.

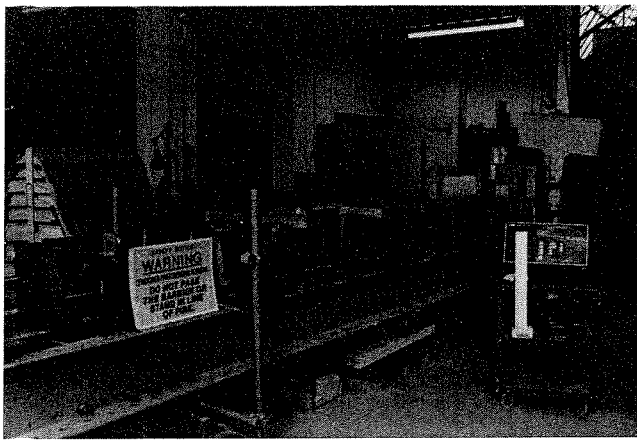


Fig. 8—Casting rig.

The manufacture of the adhesive-bonded tendons was complex, and several trials were required to optimize the procedure of applying the adhesive to the tendons. Visual and tactile observations of the coated tendons indicated that the coating of the braided AFRP resulted in a smooth outer surface. The coating of the spiral wound AFRP was not sufficiently thick to fully coat the outer spiral winding, so small deformations were still present on the outer coated surface. The average coated tendon diameters for the braided and spiral wound AFRPs were 4.0 and 4.5 mm, respectively.

After the necessary tendon preparations had been completed, both ends of the AFRP tendon were connected to pieces of prestress wire using the expansive cement couplers described elsewhere.<sup>10</sup> A schematic representation of this system can be found in Fig. 10. The steel-AFRP-steel tendon was stressed and anchored using standard equipment for the stressing of steel wire.

To monitor the load in the tendons during tensioning, two 5-mm strain gages were attached to each piece of the steel prestress wire. The gages were attached in parallel on either side of the tendon to mitigate the effects of any flexural strains in the steel. Strain gages were not attached to the AFRP for the following reasons:

1. Conventional strain gages have a maximum range of 2 percent elongation. The elongation capacities of the FiBRA and Technora are 2 and 3.7 percent, respectively.
2. The strain gages would measure the strain in the resin, which would not necessarily be representative of the strain in the FRP composite.
3. The surface profiles of the AFRPs were not conducive to the attachment of gages; the diameter of the FiBRA was only 3.7 mm and the rod was braided; the diameter of the Technora was 4 mm and the rod was characterized by closely-spaced spiral wrappings.

However, the repercussion of this decision was that the tendon forces and bond stresses during testing could only be determined through a back analysis of the experimental results. Details of this analysis will be the subject of a companion paper.<sup>2</sup>

The tendons were tensioned individually, using a hand-powered PSC single-wire jack with a capacity of approximately 70 kN. The rate of tensioning was approximately 1 kN/min. The load in the tendon was monitored using the strain gages attached to the steel prestress wire. To confirm the force in the tendon, the load in the jack was also monitored, and the overall extension of the tendon noted. After the required stress level was reached, the live end of the tendon was locked off, and the procedure was repeated until all the tendons had been tensioned. Almost immediately after tensioning, the concrete beams were cast around the free length of aramid tendon located between the couplers. By this time, the stress level in the tendons

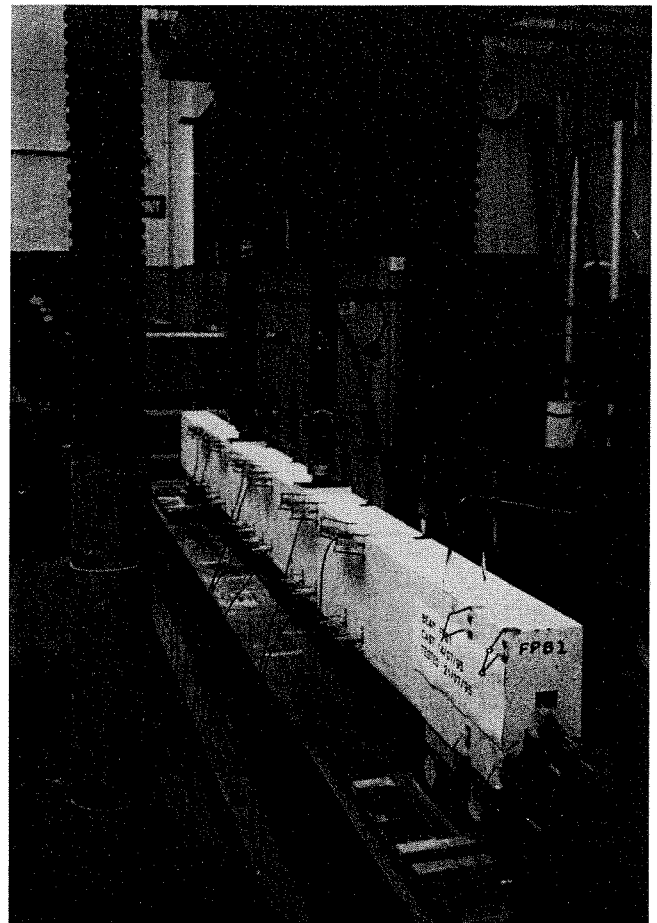


Fig. 9—Testing rig.

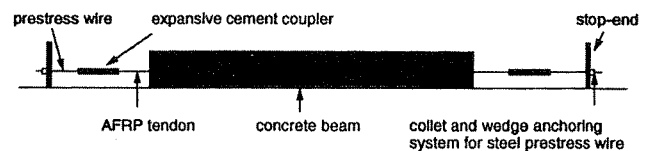


Fig. 10—Diagram of stressing system using expansive cement couplers (schematic).

had dropped to approximately 65 percent of the manufacturer's assured load, primarily as a result of a large short-term relaxation associated with the AFRP materials.

The concrete was batched in the laboratory using a pan mixer, and two batches were required for each set of beams. Three concrete cubes (100 x 100 mm), two concrete cylinders (100 x 200 mm) and two modulus-of-rupture specimens (100 x 100 x 500 mm) were cast from each batch.

After casting, the beams were covered with polythene sheet and left in the mold for 3 days. The formwork was then removed and the necessary gages attached. The beams were typically detensioned 5 days after casting, and the average concrete cube strength was found to be 55 MPa at transfer. Prior to transfer, the prestress levels in the tendons were, in general, approximately 63 to 65 percent of the manufacturers' assured loads.

### Testing of beams

In most cases, testing was carried out 7 days after casting. Portal gages were attached along the length of the beam to measure the strains at set positions. Linear variable displacement transducers (LVDTs) were used to monitor the displacements

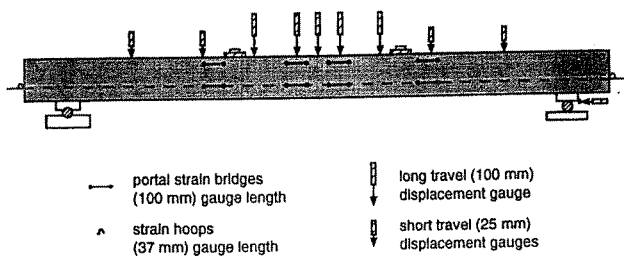


Fig. 11—Experimental gages for beam tests (schematic).

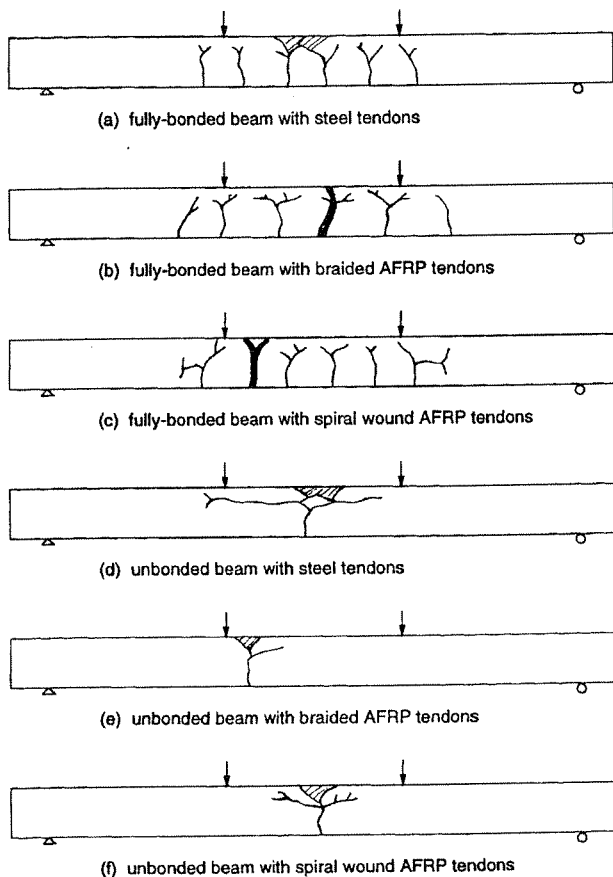


Fig. 12—Crack patterns: fully-bonded and unbonded beams (schematic).

of the beam. Strain hoops to measure slip were connected at either end of the tendons, and load cells were placed under the jacks (Fig. 11). The electronic gaging equipment was monitored using a data-logger, and the time when a reading was taken was manually controlled. In addition, the crack patterns were visually noted and the patterns monitored throughout testing. The beams were loaded monotonically until failure.

The control specimens were tested on the same day as the beams. In several cases, displacement-control tests were carried out on the concrete cylinders to ascertain the concrete stress-strain relationships. The value of the modulus of elasticity for the specimens varied between 21,000 and 22,500 MPa. The average modulus of elasticity  $E_c$  was 22,000 MPa, and the average strain at the ultimate load  $\epsilon_{cu}$  was approximately 0.0030.

As it was not possible to directly measure the prestress in the AFRP tendons, the force in the coupled steel prestress wire at the time of detensioning (Day 5) had to be extrapolated to estimate the force in the AFRP tendons at the time of testing (Day 7). Preliminary calculations suggested that the total losses due to concrete creep, concrete shrinkage, and tendon relaxation were small (1.6 percent for FIBRA, and 1.2 percent for Techno-

ra). Hence, the prestress force at the time of detensioning was taken to be representative of the level of prestress at the time of testing, without introducing a significant loss of accuracy.

## EXPERIMENTAL RESULTS

During the testing of the beams, both the cracking and the load-deflection behavior were monitored.

### Crack patterns and behavior

In the AFRP beams, as a crack formed, it grew almost instantaneously to a height of approximately 140 mm above the base of the beam. The crack growth in the steel beams was much less dramatic, and immediately after a crack occurred, the crack height was between 40 and 60 mm above the base of the beam. The rapid crack growth occurred in all the AFRP beams and was attributed to the low modulus of elasticity of the aramid tendons. The crack patterns for each beam series were quite distinct.

The cracks in the fully-bonded series were fairly uniformly distributed. Fork-like patterns were noted in the cracks in the constant moment region, whereas the cracks that occurred in the shear span tended not to fork but to propagate towards the load points [Fig. 12(a) to (c)].

The unbonded series was notable in that usually only a single crack occurred in each beam [Fig. 12 (d) to (f)]. In the beams with either steel- or spiral-wound AFRP tendons, the crack occurred close to the centerline of the beam. In the beam with braided AFRP tendons, the crack was offset 300 mm from the beam centerline. After the occurrence of the first crack, extensive horizontal cracking was noted with increasing load.

In both the first intermittently-bonded series (where the bond was expected to break down during testing) and the second intermittently-bonded series (where the bond was not expected to break down during testing), three cracks occurred in the AFRP beams [Fig. 13(a) to (d)].

Qualitatively, the greatest differences between the two types of AFRP beam behaviors were noted in the adhesive-bonded beams [Fig. 13 (e) to (f)]. In the spiral-wound AFRP beam, the central crack occurred at the crack inducer and, as the load increased, a second crack formed. However, no further cracks occurred, and it was found that the second crack closed upon subsequent loading. A minimal amount of rotation took place at the second crack and the behavior was similar to that of the unbonded beams as the beam approached failure. In contrast, the braided AFRP beam cracked in three places with large rotations occurring at each crack location. All three cracks occurred in the constant moment region.

### Ultimate loads

The ultimate loads and failure modes for the experimental beams can be found in Table 2. The load  $P_u$  represents the applied load, in excess of the beam dead-weight, that resulted in the failure of the beam. The concrete compressive cube strength and the concrete tensile strength are denoted by  $f_{cu}$  and  $f_t$ , respectively.

It should be noted that the fully-bonded AFRP beams failed due to tendon rupture. In contrast, the unbonded AFRP beams failed at a lower load due to concrete crushing. Half of the partially-bonded beams failed due to concrete crushing (TIB1, FIB1, and TAB).

There was one partially-bonded case where failure was due to the tendons rupturing (FIB2), and two cases where concrete crushing and tendon rupture appeared to occur simultaneously (TIB2 and FAB). The failure of both the concrete and the tendon at the same time would represent the most efficient use of the composite.

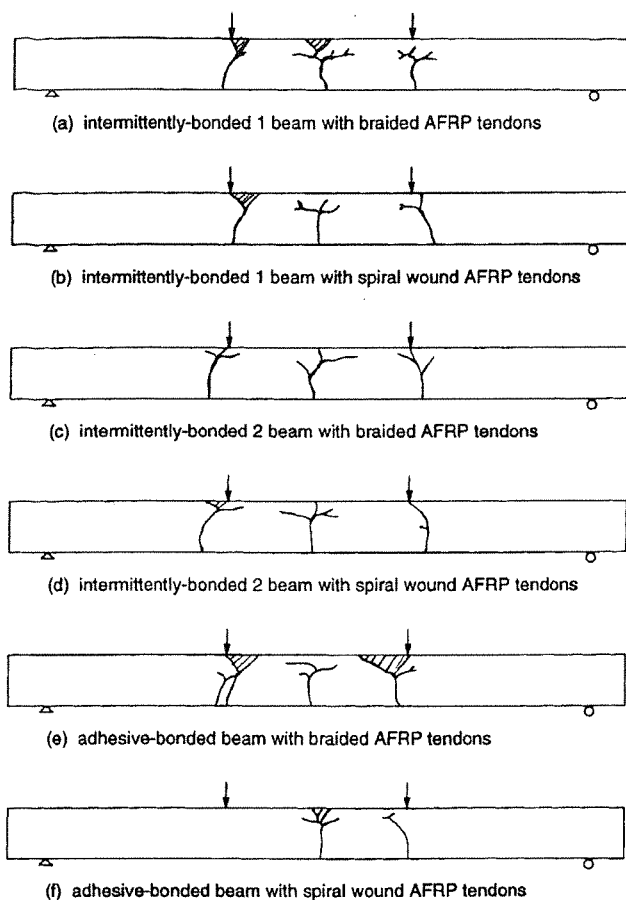


Fig. 13—Crack patterns: partially-bonded beams (schematic).

### Load-deflection curves

The load-deflection curves for the AFRP beams can be found in Fig. 14. A drop-off in load was noted after the occurrence of each crack.

### DISCUSSION OF BEAM BEHAVIOR

During the testing of the fully-bonded beams, a noticeable curvature was observed through the constant moment region. Numerous cracks occurred, but the rotation at each crack location was limited. The ultimate capacity of these beams was high, as failure was due to tendon rupture. However, only a small amount of deflection had taken place prior to the brittle failure.

In the unbonded beams, large deflections were exhibited (approximately twice those of the fully-bonded beams). The crack in the constant moment region acted as a hinge, and the sections of beam on either side of the crack behaved as rigid bodies. However, high localized strains were generated in the concrete at the hinge location, and final failure was due to the premature concrete crushing at the hinge. The ultimate load capacity was 25 percent lower than that of the fully-bonded beams.

In all cases, the deflections of the partially-bonded beams were greater than those of the fully-bonded beams and, with the exception of the adhesive-bonded beam with spiral-wound AFRP tendons, the partially-bonded beams had higher ultimate load capacities than the unbonded beams. As in the unbonded beams, the flexural cracks seemed to act as hinge locations, and the sections of beams connected by the hinges appeared to behave as rigid blocks. The formation of multiple cracks was a crucial element in insuring the enhancement of the rotation capacity of these beams. Furthermore, the development of cracks was intrinsically connected to the extent and distribution of the bond along the tendon. After first cracking, the occurrence of the second crack was a function of the mag-

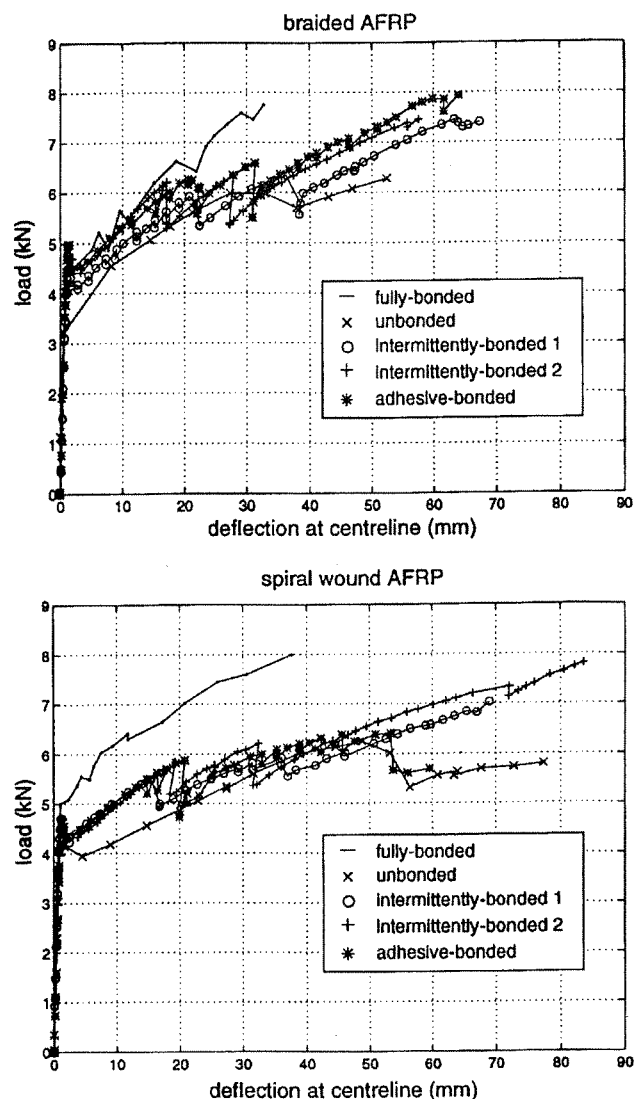


Fig. 14—Load-deflection curves for AFRP beams.

Table 2—Experimental results: ultimate loads

Beam	Prestress, kN	$f_{cu}$ , MPa	$f_t$ , MPa	$P_u$ , kN	Fail mode
SB (1)	42.5	67.8	3.1	10.4	Conc
SB (2)	44.4	70.9	3.1	10.1	Conc
TB (1)	30.7	58.5	3.0	8.0	Tendon
TB (2)	31	58.5	3.0	8.0	Tendon
FB	28	68.5	3.2	7.8	Tendon
SUB (1)	49.9	60.3	3.9	9.8	Conc
SUB (2)	46.3	65.6	3.7	9.6	Conc
TUB	28.4	60.3	3.3	6.2	Conc
FUB	29.8	60.3	3.3	6.3	Conc
TIB1	29.3	56	3.4	7.0	Conc
TIB2	29.3	56.3	3.1	7.8	Tendon/Conc
FIB1	29.1	56	3.4	7.4	Conc
FIB2	30.5	56.3	3.1	7.4	Tendon
TAB	29.1	58	3.2	6.4	Conc
FAB	30.1	58	3.2	7.9	Tendon/Conc

Note: Each beam is identified by a series of letters and, in some cases, a number. First letter indicates type of tendon material; next set of characters identifies tendon bond condition; and number in parentheses distinguishes between several beams of same type. S: 5 mm steel prestress wire; T: 4 mm spiral-wound AFRP rod; F: 3.7 mm braided AFRP rod; B: fully bonded; UB: unbonded; IB 1 or 2: intermittently-bonded Series 1 or 2; AB: adhesive bonded; Tendon: tendon breaking; and Conc: concrete crushing.



nitude of force that the tendon could transmit to the concrete through the bonded sections. If this force was less than a critical value, then second cracking did not occur. An overview of aspects of the interaction between the cracking behavior and the tendon force are detailed elsewhere.<sup>13</sup>

One potential drawback to a lesser number of cracks in the partially-bonded beam (when compared with the fully-bonded beams) is that there will possibly be less evidence of pending failure. However, after the formation of a crack, the subsequent rotations of the partially-bonded beams were higher than those of the fully-bonded beams. Hence, the presence of fewer visible cracks would be compensated by larger deflections. A key feature of the partially-bonded system is that the large rotations are a characteristic of the ultimate limit state design. Under service loading, the beam would be expected to remain uncracked.

As discussed earlier, the current work focused on the rotation capacity of the beams and did not directly address the question of ductility. To quantify the proportion of inelastic energy in the system, it would be necessary to unload the beams immediately prior to failure, and to measure the extent of the inelastic deformation. From the inelastic deformation, one could then postulate both the total and elastic energy in the system. Unfortunately, as it is often difficult to predict the failure load, finding the exact point at which to unload is problematic; hence, load-cycling is required. In addition, Vijay et al.<sup>14</sup> found that, in beams that failed by concrete crushing, the inelastic energy was highly dependent on the stage at which the load was released at the onset of the compressive failure.

In partially-bonded beams, it is expected that the total energy input into the system will result in a combination of the following actions: the extension of the tendon; the straining of the concrete in compression; possible dowel action; the formation of cracks in the concrete; aggregate interlock; the debonding of the tendon from the concrete and the frictional bond resistance. As the beams were tested monotonically until failure, it is not possible to make definitive statements about the relative amounts of elastic and inelastic energy (the residual inelastic deformations were not measured). However, it is important to note that the tendon extension is linearly elastic (except for possibly a small amount of creep) and it is expected that this will be a dominant component of the total energy of the system. Some inelastic energy will be dissipated in the concrete, hence, the beams that exhibited large rotations are likely to have a higher plastic energy absorption than the beams with small rotation capacities. The possibility of enhancing this energy absorption is the subject of current research.

From the experimental results, it can be seen that the concept of partial bond has far-reaching implications for the flexural design of concrete pretensioned with FRP tendons (a discussion of these implications can be found elsewhere<sup>15</sup>). By controlling the bond at particular locations along the beam, the designer can optimize both the ultimate capacity and the rotation capacity of a beam.

Although the principle of partial bond is promising, further work is necessary to insure the long-term performance of the system. Additional areas requiring investigation would include: the fatigue behavior of the intermittently and adhesive-bonded beams; the long-term integrity of the bond; and the effect of the intermittent or the adhesive bond on the shear capacity of the beam.

## CONCLUSIONS

The energy considerations in an FRP-prestressed beam are very different from those of a similar beam with steel tendons. There is little ductility in FRP systems, thus, the rotation capacity of these systems is of great importance. Failure due to tendon rupture is brittle and sudden.

In the main experimental series, small-scale (100 x 200 x 2800 mm) fully-bonded, unbonded, and partially-bonded pretensioned concrete beams were cast. The beams were tested under four-point loading until failure. The fully-bonded beams had a high ultimate load capacity and failed due to tendon rupture. However, only limited rotations occurred prior to failure. During the testing of the unbonded beams, a single crack formed and, though large rotations were apparent, premature failure occurred due to concrete crushing. The ultimate load capacity of the unbonded beams was significantly lower (by 25 percent) than that of the fully-bonded beams.

The partially-bonded beam tests were extremely successful and, with the exception of the adhesive-bonded beam with spiral-wound AFRP tendons, all the partially-bonded beams had a high ultimate load capacity and a large rotation capacity. The beams appeared to act as a series of rigid blocks connected by hinges, and the formation of multiple cracks was a crucial element in insuring that premature concrete crushing did not occur (as evidenced in the unbonded beams). In two of the beams—the adhesive-bonded braided AFRP beam and the second intermittently-bonded spiral-wound AFRP beam—an ultimate load capacity equivalent to that of the fully-bonded beams was achieved. It was demonstrated that the idea of partial bonding could be used to optimize the flexural response of concrete beams pretensioned with FRP tendons.

## ACKNOWLEDGMENTS

The authors are grateful for the support of Chichibu Onoda Cement Co., Teijin Ltd., Mitsui Construction Co., and Tarmac Precast Concrete Ltd. Kevlar is a trade name of DuPont, Technora of Teijin, and FiBRA of Mitsui. Janet M. Lees was sponsored by the Natural Sciences and Engineering Research Council of Canada (NSERC) and is appreciative of its financial assistance.

## NOTATIONS

$B$	= bonded segment
$E_c$	= modulus of elasticity of concrete
$E_t$	= modulus of elasticity of tendon
$f_{cu}$	= concrete compressive cube strength
$f_t$	= modulus of rupture tensile strength of concrete
$L_{ab}$	= bond breakdown length of adhesive bonded tendon
$L_b$	= bonded length of tendon segment
$L_{ub}$	= unbonded length of tendon segment
$P_o$	= initial prestress force
$P_u$	= ultimate applied load
$P_{ult}$	= manufacturer's assured load for tendon
$T$	= force in tendon segment
$UB$	= unbonded segment
$V_f$	= volume fraction of fibers
$\beta$	= angle relating to the change in force with length
$\epsilon_{cu}$	= ultimate concrete compressive strain at failure
$\phi$	= bar diameter

## REFERENCES

1. Burgoyne, C. J., "Should Fiber Reinforced Plastic be Bonded to Concrete?" *Fiber Reinforced Plastic Reinforcement for Concrete Structures*, A. Nanni and C. W. Dolan, eds., SP-138, American Concrete Institute, Farmington Hills, Mich., 1993, pp. 367-380.
2. Lees, J. M., and Burgoyne, C. J., "Analysis of Concrete Beams with Partially-Bonded Composite Reinforcement." (submitted to ACI for publication)
3. Nanni, A. et al., "Tensile Properties of Braided Fiber Reinforced Plastic Rods for Concrete Reinforcement," *Cement & Concrete Composites*, V. 15, No. 3, 1993, pp. 121-129.
4. Noritake, K. et al., "Technora—An Aramid Fiber Reinforced Plastic Rod," *Fiber Reinforced Plastic (FRP) Reinforcement for Concrete Structures: Properties and Applications*, A. Nanni, ed., Developments in Civil Engineering, 42, Elsevier Science Publishers B. V., 1993, pp. 267-290.
5. Mera, H., and Takata, T., "High-Performance Fibers," *Ullmann's Encyclopedia of Industrial Chemistry*, V. A. 13, VCH, 5th edition, 1989.
6. Teijin Ltd., "High-Tenacity Aramid Fiber—Technora," *Technical Information—TIE-05/89.11*, 1989.
7. Tamura, T., "FiBRA," *Fiber Reinforced Plastic (FRP) Reinforcement for Concrete Structures: Properties and Applications*, A. Nanni, ed., Developments in Civil Engineering, 42, Elsevier Science Publishers B. V., 1993, pp. 291-303.
8. Tanigaki, M. et al., "Study of Braided Aramid Fiber Rods for Rein-



forcing Concrete," *JABSE*, 13th Conference, Helsinki, 1988, pp. 15-20.

9. Kakihara, R. et al., "A New Aramid Rod for the Reinforcement of Prestressed Concrete Structures," *Advanced Composite Materials in Civil Engineering Structures Proceedings*, MT Division/ASCE, Las Vegas, Jan. 1991, pp. 132-142.

10. Lees, J. M.; Gruffydd-Jones, B.; and Burgoyne, C. J., "Expansive Cement Couplers—A Means of Pretensioning Fiber Reinforced Plastic Tendons," *Construction and Building Materials*, V. 9, No. 6, 1995, pp. 413-423.

11. Gerritse, A., "Specific Features and Properties of Aramid Fiber Reinforced Plastic Bars," *Advanced Composite Materials in Bridges and Structures—2nd International Conference*, M. M. El-Badry, ed., Canadian Society of Civil Engineering, Montreal, Aug. 11-14, 1996, pp. 75-82.

12. Lees, J. M., "Flexure of Concrete Beams Pretensioned with Aramid Fiber Reinforced Plastics," PhD thesis, Department of Engineering, University of Cambridge, UK, 1997.

13. Lees, J. M., and Burgoyne, C. J., "Rigid Body Analysis of Concrete Beams Pretensioned with Partially-Bonded Aramid Fiber Reinforced Plastic Tendons," *Nonmetallic Fiber Reinforced Plastic (FRP) Reinforcement for Concrete Structures*, Proceedings of the Third International Symposium, Sapporo, Japan, V. 2, Japan Concrete Institute, Oct. 1997, pp. 759-766.

14. Vijay, P. V.; Kumar, S. V.; and GangaRao, H. V. S., "Shear and Ductility Behavior of Concrete Beams Reinforced with Glass Fiber Reinforced Plastic Reinforcing Bars," *Advanced Composite Materials in Bridges and Structures—2nd International Conference*, M. M. El-Badry, ed., Canadian Society of Civil Engineering, Montreal, Aug. 1996, pp. 217-226.

15. Burgoyne, C. J., "Rational Use of Advanced Composites in Concrete," *Nonmetallic Fiber Reinforced Plastic (FRP) Reinforcement for Concrete Structures*, Proceedings of the Third International Symposium, Sapporo, Japan, V. 2, Japan Concrete Institute, Oct. 1997, pp. 75-88.

